Recursive-Green's-function analysis of wave propagation in two-dimensional nonhomogeneous media

K. B. Kahen
Research Laboratories, Eastman Kodak Company, Rochester, New York 14650-2216
(Received 30 November 1992)

An alternative method is presented for computing wave propagation in two-dimensional nonhomogeneous media. The method is based on computing the exact Green's function for a domain using a recursive Green's-function approach. In comparison with the finite-difference time-domain method, our approach requires substantially less memory and computational time, enabling the modeling of larger and more complex domains. The method is validated by comparing with exact analytical solutions and is found to be highly accurate.

PACS number(s): 42.25.Bs, 41.20.Jb, 02.70.+d, 42.25.Fx

I. INTRODUCTION

Wave propagation in nonhomogenous media has been an active area of study in many fields over the years [1–10] with emphasis on different computational tools depending on the specific application. For integrated-optics devices, the problem domains are large, while, generally, the beam divergences are small and the index of refraction is a weak function in the direction of propagation. The latter two properties can be exploited to simplify the solution of the Helmholtz equation. To this end, various marching algorithms, under the generic title of the beam-propagation method (BPM), have been developed to study forward-propagating solutions within these devices [1–3]. Recently, the BPM has been extended to include reflections (bidirectional BPM [4]) and exact forward-propagating solutions [5]. However, the bidirectional BPM cannot efficiently model gratings and loses accuracy for strongly guided devices, while the exact solution of the Helmholtz equation using the Lanczos method is very slow for strongly guided structures. In the field of electromagnetic wave scattering, the general approach has been the direct solution of either the time-independent [6,7] or time-dependent Maxwell's equations [8–10]. For example, the finite-element and boundary-element methods have been combined to model discontinuities in open slab waveguides [6,7]. However, the domain of the discontinuity must be limited to avoid excessive computational times associated with the finite-element solution of the Helmholtz equation. For the time-dependent case, the technique of choice is typically the finite-difference time-domain (FDTD) method [8], which has been used to model both scattering by arbitrary obstacles [9] and gratings [10]. As for the time-independent case, the FDTD technique is very computationally intensive, thus limiting the complexity and size of the problem domain.

In order to combine the speed of the BPM with the accuracy of the FDTD method, we introduce a recursive Green's-functional solution [11,12] of the Helmholtz equation. For simplicity, the technique is applied to the solution of the two-dimensional scalar wave equation; however, it is straightforward to extend the approach to three dimensions and to solutions of the vector wave equation [13]. The recursive method is an algorithm for computing the Green's function of a large domain based on the knowledge of the Green's function of smaller sections of the domain. In each recursion step, the Green's functions corresponding to two adjoining sections are replaced by a single Green's function of the composite section. Referring to Fig. 1, the large structure of extent L_z is split up into smaller sections (to be called unit sections) of length ΔL_z, whose Green's functions can be easily computed. The recursive method is used to form the overall Green's function by building up the size of the domain section by section until it corresponds to the structure of the proper length. More specifically, starting from the left-hand side of the structure and proceeding to the right, with each successive recursion step, the left-hand section Green's function increases in complexity and thickness [from ΔL_z to $(M-1)\Delta L_z$], while the right-hand section Green's function corresponds to that of the unit section. Since ΔL_z can be on the order of nanometers, the original two-dimensional problem is effectively reduced to a series of one-dimensional problems, leading to small memory requirements and fast computational times. The unit-section Green's functions are computed by solving Dyson's equation [14] which is recast as a linear algebraic equation set. Having determined the overall Green's function, Green's theorem is used to calculate the reflected and transmitted fields, yielding the overall reflection and transmission coefficients. We previously applied this approach to computing the propagation constants of first-order one-dimensional laser cavities [12]. As for that case, the one trade-off of our recursive approach is that the field distribution within the structure cannot be determined. However, for many applications, e.g., distributed-feedback laser analysis [12], computing the internal fields is not essential and, presently, we are extending our approach to include the capability of calculating field distributions at selected longitudinal cross sections.

II. METHODOLOGY

In this section, the formalism is derived for computing the Green's function of an arbitrary two-dimensional

domain composed of complex dielectric media. In Sec. II A, the wave equation and its boundary conditions are given, followed, in Sec. II B, by a discussion of the construction of the unit-section Green's function. In Sec. II C, the recursive-Green's-function formalism is derived, while in Sec. II D, Green's theorem is used to compute the reflected and transmitted fields.

A. Wave equation

In the following it will be assumed that the transmittance and reflectance of two-dimensional complex dielectric media can be computed through the solution of the scalar Helmholtz wave equation. As shown elsewhere [13], the extension to the case of the solution of the vector wave equation is straightword. Figure 1 shows a schematic of a two-dimensional nonhomogenous domain, divided into M smaller sections for later calculation of the unit-section Green's functions. Indicted in the figure are the input, transmitted, and reflected fields, $E_i(y)$, $E_t(y)$, and $E_r(y)$, respectively. There is no incident field at $z=L_z$, since the surrounding media is assumed to extend to infinity on both sides of the structure. The schematic indicates a rectangular boundary; however, the media contained within the boundaries can assume any shape. The scalar Helmholtz wave equation can be written as

$$[\nabla_y^2+\nabla_z^2+k^2N(y,z)^2]\psi(y,z)=0 , \tag{1}$$

where ψ is the wave function (electric field), k $(=2\pi/\lambda)$ is the free-space propagation constant, and $N(y,z)$ is the complex refractive index distribution. Assuming that external to the structure the effective indices of refraction are N_0 and N_2 on the left- and right-hand sides, respectively, the boundary values for $\psi(y,z)$ can be determined based on the continuity of the electric field across dielectric interfaces,

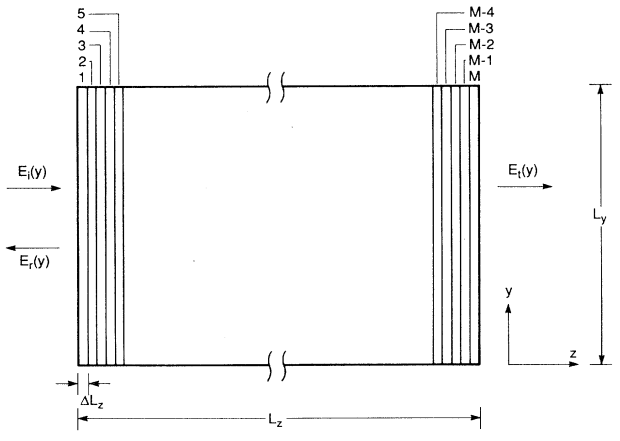

FIG. 1. Schematic of a two-dimensional nonhomogenous domain indicating the division of the structure into M smaller sections. The exact Green's function is computed for each of the sections. Also indicated are the incident, reflected, and transmitted fields, $E_i(y)$, $E_r(y)$, and $E_t(y)$, respectively.

$$\psi(y,z=0)=E_i(y)+E_r(y) , \tag{2a}$$

$$\psi(y,z=L_z)=E_t(y)e^{ikN_2L_z} . \tag{2b}$$

B. Unit-section Green's function

As indicated in Fig. 1, the rectangular domain is split up into M thinner rectangular sections of thickness ΔL_z. The motivation behind the division is that it is simpler numerically to obtain the Green's function of M thin sections, rather than one thick section of extent $M\Delta L_z$. Prior to constructing the unit-section Green's functions, it is necessary to determine their boundary conditions. This choice requires some special considerations. The most general homogeneous boundary conditions are of the form

$$AG(y,a;y'z')+B\frac{dG(y,z;y',z')}{dz}\Big|_{z=a}=0.0 , \tag{3a}$$

$$CG(b,z;y',z')+D\frac{dG(y,z;y',z')}{dy}\Big|_{y=b}=0.0 , \tag{3b}$$

where Eqs. (3a) and (3b) refer to the longitudinal (z) and transverse (y) boundaries, respectively, $G(y,z;y',z')$ is the two-dimensional Green's function, a and b denote end points for the longitudinal and transverse boundaries, respectively, and A, B, C, and D are known coefficients. The positions of the transverse boundaries are chosen such that the field is zero along it. In order to help enforce this condition, an absorbing region is employed adjacent to the $y=0,L_y$ boundaries, i.e., to the complex refractive index distribution within a distance W_a from the boundary, an imaginary contribution $n_i\cos(\pi|y-b|/2W_a)$ is added. This technique is used in both FDTD [9] and BPM [1] simulations to prevent reflections of outwardly scattered radiation back into the problem domain. Consequently, in Eq. (3b), $C=1$ and $D=0$. As will be discussed in Sec. II D, depending on the form of the longitudinal boundary conditions, Green's theorem can be used to compute the transmission coefficient either in terms of the $z=0,L_z$ Green's functions or their derivatives. As will be shown in Sec. II C, the recursive Green's function method can be used to compute easily the end point Green's functions, not their derivatives. Hence B must be nonzero, while A can assume any value [15]. Consequently, the simplest choice is $A=0$ and $B=1$. Since the boundary conditions are maintained during the recursion process, the same boundary conditions apply to each unit section.

The unit section Green's functions are determined by solving Dyson's equation (an integral equation) [14]. This is the standard approach taken in quantum field theory for computing the perturbed Green's function from the known, unperturbed Green's function and is exact. Unlike typical perturbation approaches, the perturbation does not have to be small in order to give correct results. For details concerning the derivation and usage of Dyson's equation, the reader is referred to Ref. [14]. In operator notation, Dyson's equation can be written as

$$G=G^0+G^0\{-V\}G \ , \tag{4}$$

where G^0 is the known, unperturbed Green's function, V is the perturbation, and G is the desired, perturbed Green's function. [Typically, Eq. (4) is written with no minus sign in front of the perturbation V.] Since Eq. (4) is an operator expansion, it is necessary to convert it into a specific representation. The most appropriate is the real-space representation, which yields

$$G(y,z;y'z')=G^0(y,z;y',z')+\int_0^{L_y}dy''\int_0^{\Delta L_z}dz''G^0(y,z;y'',z'')\{-V(y'',z'')\}G(y'',z'';y',z') \ , \tag{5}$$

which clearly shows that Dyson's equation is an integral equation. Prior to solving Eq. (5), it is necessary to choose G^0 and V. G^0 can be constructed analytically if it corresponds to a unit section composed of a uniform index n_a (we chose n_a to be also purely real). For a two-dimensional rectangular domain, the scalar wave equation Green's function cannot be derived in closed form, but can be represented by the following single series expansion [16]:

$$G^0(y,z';y',z')=\sum_{\rho}\frac{2\cos[C(z-z_b)\cos[C(z'-z_t)]\sin(\rho\pi y/L_y)\sin(p\pi y'/L_y)}{L_yC\sin(CL_z)} \quad (z<z') \ , \tag{6}$$

where z_t and z_b are the top and bottom longitudinal boundaries of the unit section, respectively, $C^2=k^2n_a^2-(\rho^2\pi^2/L_y^2)$, and there is an analogous expression for $z>z'$, which is obtained by reversing z and z' in the numerator. Typically, p is taken up to 400 to obtain good convergence, where if the structure has symmetry about $L_y/2$, then only odd values are necessary. It should be noted that C becomes complex for certain values of p; hence, complex cosine (or cosh) functions need to be employed. With the above choice for G^0, $V(y,z)=k^2[N^2(y,z)-n_a^2]$.

Equation (5) is typically solved by expanding in an orthonormal basis set, involving global basis functions [15]. However, as a result of the very small thickness of the unit-section rectangles (on the order of nanometers), only a minimal basis-set expansion is required in the longitudinal direction. The simplest solution is to employ a collocation basis set, i.e., use a quadrature rule to evaluate the z-dependent integrals in Eq. (5),

$$G(y,z_j;y',z_l)=G^0(y,z_j;y',z_l)+\int_0^{L_y}dy''\sum_i w_iK(y,z_j;y'',z_i)\times G(y'',z_i;y',z_l) \ , \tag{7}$$

where $K(y,z;y'',z'')=G^0(y,z;y'',z'')\{-k^2N^2(y'',z'')\}$, and z_i and w_i are the quadrature points and weights at point i, respectively. As a result of the extent of ΔL_z, only three quadrature points were required and the weights were chosen according to Simpson's rule. In the transverse direction it was determined that expanding in global basis functions resulted in Eq. (7) converging very slowly. The simplest one-dimensional localized, nonorthonormal basis functions are overlapping chapeau functions, $\phi_m(y)$ [17]. Upon expanding Eq. (7) in $\phi_m(y)$, one obtains

$$\sum_{p,q}g_{pq}(z_j,z_l)\phi_p(y)\phi_q(y')=\sum_{p,q}g^0_{pq}(z_j,z_l)\phi_p(y)\phi_q(y')+\int_0^{L_y}dy''\sum_{i,p,n}w_iK_{pn}(z_j,z_i)\phi_p(y)\phi_n(y'')\sum_{m,q}g_{mq}(z_i,z_l)\phi_m(y'')\phi_q(y') \ , \tag{8}$$

where, for example, K_{pn} is a $(m_{\text{bas}}\times 3)\times(m_{\text{bas}}\times 3)$ matrix and m_{bas} is the number of $\phi_m(y)$ basis functions (there are three collocation basis functions). Following integration over y'' and some straightforward manipulation, one obtains

$$\sum_{i,m}[\delta_{ij}\delta_{pm}-\sum_n w_iK_{pn}(z_j,z_i)S_{nm}]g_{mq}(z_i,z_l)=g^0_{pq}(z_j,z_l) \ , \tag{9a}$$

$$S_{nm}=\int_0^{L_y}dy\ \phi_n(y)\phi_m(y) \ , \tag{9b}$$

where S is the $\phi_m(y)$ overlap matrix and Eq. (9a) is a set of linear algebraic equations ($Ax=b$). Prior to solving Eq. (9a) for g, it is necessary to determine expressions for $g^0_{pq}(z_j,z_l)$ and $K_{pn}(z_j,z_i)S_{nm}$. Since $g^0_{pq}(z_j,z_l)$ is the transform of $G^0(y,z_j;y',z_l)$, it is simple to show that

$$g^0_{pq}(z_j,z_l)=\sum_{m,n}S^{-1}_{pm}\left[\int_0^{L_y}dy\int_0^{L_y}dy'\phi_m(y)G^0(y,z_j;y',z_l)\times\phi_n(y')\right]S^{-1}_{nq} \ , \tag{10}$$

where a comparable expression for $K_{pn}(z_j,z_i)S_{nm}$ can be analogously derived. As a result of employing chapeau

basis functions, the integrals in Eq. (10) are straightforward to evaluate.

C. Recursive-Green's-function formalism

The recursive-Green's-function method was introduced previously [11] to study the transmission properties of electrons through disordered samples. The formalism can be generated through repeated application of Dysons' equation. In order to help clarify the derivation for optical wave propagation, reference will be made to Fig. 2(a), which illustrates two sections of a composite domain, S_1 and S_2, having longitudinal lengths L_1 and L_2-L_1, respectively, and complex indices of refraction, n_1 and n_2 (which can be nonuniform), respectively. As will be discussed below in Sec. II D, the calculation of $E_r(y)$ and $E_t(y)$ requires that the overall Green's function be evaluated at $g(0,0)$, $g(0,L)$, $g(L,0)$, and $g(L,L)$, where each g is an $(m_{\text{bas}}\times m_{\text{bas}})$ matrix. Consequently, in computing the Green's function of the composite domain indicated in Fig. 2(a), $g(0,0)$, $g(L_2,0)$, $g(0,L_2)$, and $g(L_2,L_2)$ needed to be evaluated. In order to calculate the composite domain Green's function using Dyson's equation, a perturbation must be constructed that links the two sections of the domain. Consequently, in Fig. 2(b), the composite domain is redrawn so that section S_1 now extends to $L_1'=L_1+\varepsilon$, and $V(y,z)=k^2(n_2^2-n_1^2)$ between L_1 and L_1'; while in Fig. 2(c), section S_1 extends to $L_1''=L_1-\varepsilon$ and $V(y,z)=k^2(n_1^2-n_2^2)$ between L_1'' and L_1. Figures 2(b) and 2(c) are to be used when the unperturbed sections (as per Dyson's equation) are S_1 and S_2, respectively. Prior to applying Eq. (5), boundary conditions must be set and G^0 needs to be calculated. The boundary conditions are those specified in Sec. II B. For the first recursion step, G^0 for both S_1 and S_2 is the unit-section Green's function. For the nth recursion step, G^0 for S_2 is the same, while G^0 for S_1 is computed in the $(n-1)$th recursion step.

$G(0,L_2)$ and $G(L_2,L_2)$ can be derived from the following set of equations:

$$G(y,0;y',L_2)=\int_0^{L_y}dy''\int_{L_1}^{L_{1'}}dz\,G^0_{n_1}(y,0;y'',z)[-V(y'',z)]G(y'',z;y',L_2)\,, \tag{11a}$$

$$G(y,L_2;y',L_2)=G^0_{n_2}(y,L_2;y',L_2)+\int_0^{L_y}dy''\int_{L_{1''}}^{L_1}dz\,G^0_{n_2}(y,L_2;y'',z)[V(y'',z)]G(y'',z;y',L_2)\,, \tag{11b}$$

$$G(y,L_1;y',L_2)=G^0_{n_2}(y,L_1;y',L_2)+\int_0^{L_y}dy''\int_{L_{1''}}^{L_1}dz\,G^0_{n_2}(y,L_1;y'',z)[V(y'',z)]G(y'',z;y',L_2)\,, \tag{11c}$$

$$G(y,L_1;y',L_2)=\int_0^{L_y}dy''\int_{L_1}^{L_{1'}}dz\,G^0_{n_1}(y,L_1;y'',z)[-V(y'',z)]G(y'',z;y',L_2)\,, \tag{11d}$$

where, for example, $G^0_{n_1}$ indicates the isolated domain Green's function for S_1. Note that Eqs. (11a) and (11d) were derived with reference to Fig. 2(b), while the other two equations were based on Fig. 2(c); hence the two different expressions for $G(y,L_1;y',L_2)$. Additionally, in Eqs. (11a) and (11d) there are no isolated $G^0_{n_1}$ contributions for $G(y,0;y',L_2)$ and $G(y,L_1;y',L_2)$, since the two observations points $(0,L_2$ and $L_1,L_2)$, respectively, exist on different sides of the discontinuity. Since the discontinuity was introduced as a device to enable us to make use of Dyson's equation, the limit needs to be taken as the extent of the perturbation region goes to zero, i.e., $V(y'',z)\to V(y'',L_1)\delta(z-L_1)$,

$$G(y,0;y',L_2)=\int_0^{L_y}dy''G^0_{n_1}(y,0;y'',L_1)[-V(y'',L_1)]G(y'',L_1;y',L_2)\,, \tag{12a}$$

$$G(y,L_2;y',L_2)=G^0_{n_2}(y,L_2;y',L_2)+\int_0^{L_y}dy''G^0_{n_2}(y,L_2;y'',L_1)[V(y'',L_1)]G(y'',L_1;y',L_2)\,, \tag{12b}$$

$$G(y,L_1;y',L_2)=G^0_{n_2}(y,L_1;y',L_2)+\int_0^{L_y}dy''G^0_{n_2}(y,L_1;y'',L_1)[V(y'',L_1)]G(y'',L_1;y',L_2)\,, \tag{12c}$$

$$G(y,L_1;y',L_2)=\int_0^{L_y}dy''G^0_{n_1}(y,L_1;y'',L_1)[-V(y'',L_1)]G(y'',L_1;y',L_2)\,. \tag{12d}$$

After expanding Eq. (12) in the $\phi_m(y)$ basis set, integration over y'' is performed, followed by some simple manipulations to obtain

$$g_{pq}(0,L_2)=-\sum_{m,n}(g^0_{n_1})_{pm}(0,L_1)V_{mn}(L_1)g_{nq}(L_1,L_2)\,, \tag{13a}$$

$$g_{pq}(L_2,L_2)=(g^0_{n_2})_{pq}(L_2,L_2)+\sum_{m,n}(g^0_{n_2})_{pm}(L_2,L_1)\times V_{mn}(L_1)g_{nq}(L_1,L_2)\,, \tag{13b}$$

$$g_{pq}(L_1,L_2)=(g^0_{n_2})_{pq}(L_1,L_2)+\sum_{m,n}(g^0_{n_2})_{pm}(L_1,L_1)\times V_{mn}(L_1)g_{nq}(L_1,L_2)\,, \tag{13c}$$

$$g_{pq}(L_1,L_2)=-\sum_{m,n}(g^0_{n_1})_{pm}(L_1,L_1)V_{mn}(L_1)g_{nq}(L_1,L_2)\,, \tag{13d}$$

$$V_{mn}(L_1)=\int_0^{L_y}dy''\phi_m(y'')V(y'',L_1)\phi_n(y'')\,. \tag{13e}$$

By equating Eqs. (13c) and (13d), an expression for

$g_{pq}(L_1,L_2)$ can be obtained in terms of known quantities,

$$g(L_1,L_2)=-V(L_1)^{-1}[g^0_{n_1}(L_1,L_1)+g^0_{n_2}(L_1,L_1)]^{-1} \times g^0_{n_2}(L_1,L_2) , \quad (14)$$

where the subscript notation was dropped (all quantities are matrices). Finally, upon substituting the above expression for $g(L_1,L_2)$ into Eqs. (13a) and (13b), the desired relations are obtained,

$$g(0,L_2)=g^0_{n_1}(0,L_1)T(L_1,L_1)g^0_{n_2}(L_1,L_2) , \quad (15a)$$

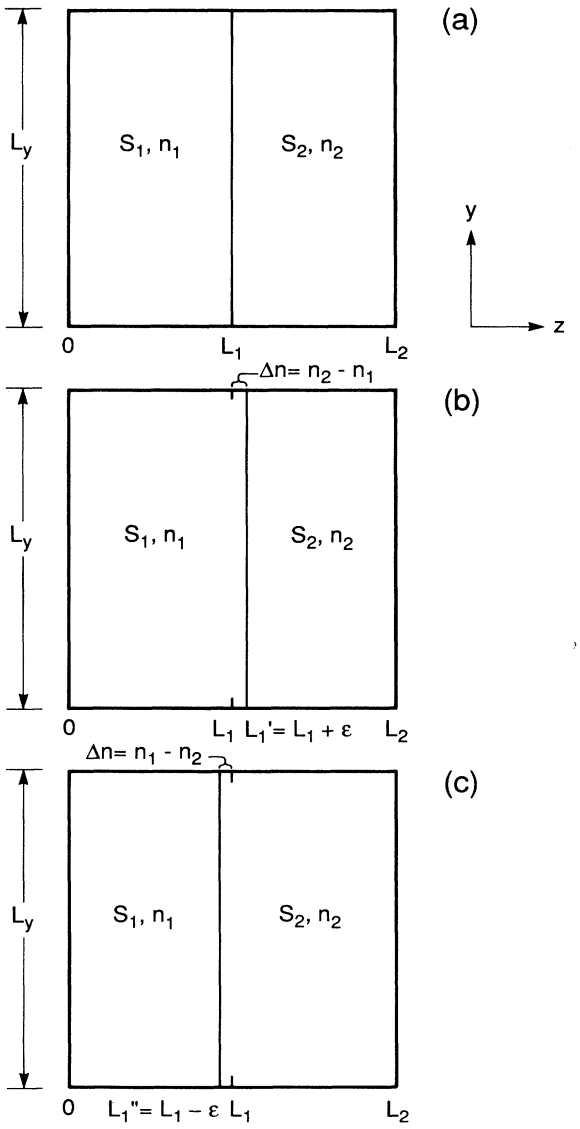

FIG. 2. Schematic of a two-section composite domain. In the two sections S_1 and S_2, the indices of refraction are equal to n_1 and n_2, respectively. (a) The longitudinal lengths of S_1 and S_2 are L_1 and L_2-L_1, respectively. In order to make avail of Dyson's equation, the domain is modified as in (b) and (c). In (b), S_1 is increased in thickness to $L_1+\varepsilon$, and $\Delta n=n_2-n_1$; while, in (c), S_1 is decreased in thickness to $L_1-\varepsilon$, and $\Delta n=n_1-n_2$.

$$g(L_2,L_2)=g^0_{n_2}(L_2,L_2) - g^0_{n_2}(L_2,L_1)T(L_1,L_1)g^0_{n_2}(L_1,L_2) , \quad (15b)$$

$$T(L_1,L_1)=[g^0_{n_1}(L_1,L_1)+g^0_{n_2}(L_1,L_1)]^{-1} . \quad (15c)$$

where both expressions are functions of known quantities, are independent of V, and defined in terms of the t-matrix T, which acts as an effective potential to link the two sections. By going through an analogous procedure, the following expressions for $g(0,0)$ and $g(L_2,0)$ can be derived:

$$g(0,0)=g^0_{n_1}(0,0)-g^0_{n_1}(0,L_1)T(L_1,L_1)g^0_{n_1}(L_1,0) , \quad (16a)$$

$$g(L_2,0)=g^0_{n_2}(L_2,L_1)T(L_1,L_1)g^0_{n_1}(L_1,0) . \quad (16b)$$

In comparison with our one-dimensional recursion relations [12], the two sets of expressions are analogous except for the above quantities being matrices instead of scalars. Using Eqs. (15) and (16), one can start from the left-hand side of the domain and recursively add one unit section at a time to the current structure until the total domain is simulated.

D. Field evaluation

As is well known [16], Green's theorem can be used to evaluate the wave function anywhere inside a defined domain in terms of the boundary values and derivatives of the wave function and its corresponding Green's function. By an appropriate choice of boundary conditions [15], the dependence on the Green's function derivatives can be eliminated. One particular choice that realizes this situation was made in Sec. II B and the resulting expression for the wave functions along the $z=0,L_z$ boundaries is

$$\psi(y,z=0,L_z)=\int_0^{L_y}dy'G(y',0;y,z)X(y',0) - \int_0^{L_y}dy'G(y',L_z;y,z)X(y',L_z) , \quad (17a)$$

$$X(y,z)=\frac{\partial\psi(y,z)}{\partial z} , \quad (17b)$$

where $X(y,z=0,L_z)$ can be evaluated using Eq. (2) and the continuity of the electric-field derivative across dielectric interfaces. Upon expanding the y dependences of both the Green's functions and X in the $\phi_m(y)$ basis set and integrating over y', one obtains for the $z=L_z$ boundary,

$$\sum_p (E_t)_p\phi_p(y)=ikN_0\sum_{m,n,p}\phi_m(y)g_{mn}(0,L_z) \times S_{np}[(E_i)_p-(E_r)_p] - ikN_2\sum_{m,n,p}\phi_m(y)g_{mn}(L_z,L_z) \times S_{np}(E_t)_p , \quad (18)$$

where, for example, $(E_t)_p$ are the coefficients for the $\phi_m(y)$ expansion of E_t. After multiplying both sides of

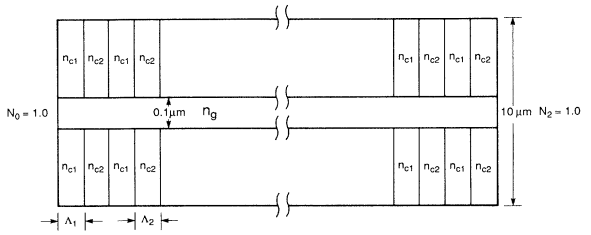

FIG. 3. Schematic of a 200 period first-order distributed-feedback reflector composed of a volume grating.

Eq. (18) by $\int_0^{L_y} dy\, \phi_q(y)$, performing the integration, and collecting like terms, one obtains

$$[I+ikN_2 g(L_z,L_z)S]E_t - ikN_0[g(0,L_z)S]E_i + ikN_0[G(0,L_z)S]E_r = 0 , \quad (19a)$$

$$ikN_2[g(L_z,0)S]E_t + [I - ikN_0 g(0,0)S]E_i + [I + ikN_0 g(0,0)S]E_r = 0 , \quad (19b)$$

where I is the identify matrix, the subscripts have been dropped, and Eq. (19b) was obtained in an analogous fashion for the $z=0$ boundary. The above matrix-vector equation set is straightforward to solve for both E_t and E_r in terms of E_i. Finally, upon back transforming, one obtains the desired quantities, $E_t(y)$ and $E_r(y)$.

III. RESULTS

In order to check the accuracy of our approach we simulated wave propagation through a volume grating, as illustrated in Fig. 3, and through a 3-μm slit (to model single-slit diffraction). The reason for choosing these two problems is that analytical solutions exist [18] and the amount of out-scattered radiation is minimal; hence

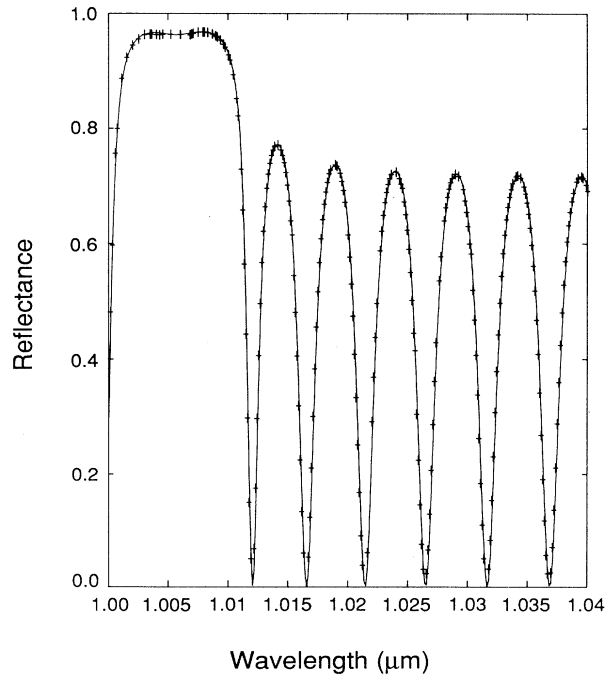

FIG. 4. Reflectance of a 200 period first-order distributed-feedback reflector as a function of wavelength. The solid lines are the exact analytical results, while the crosses are the Green's functional calculations.

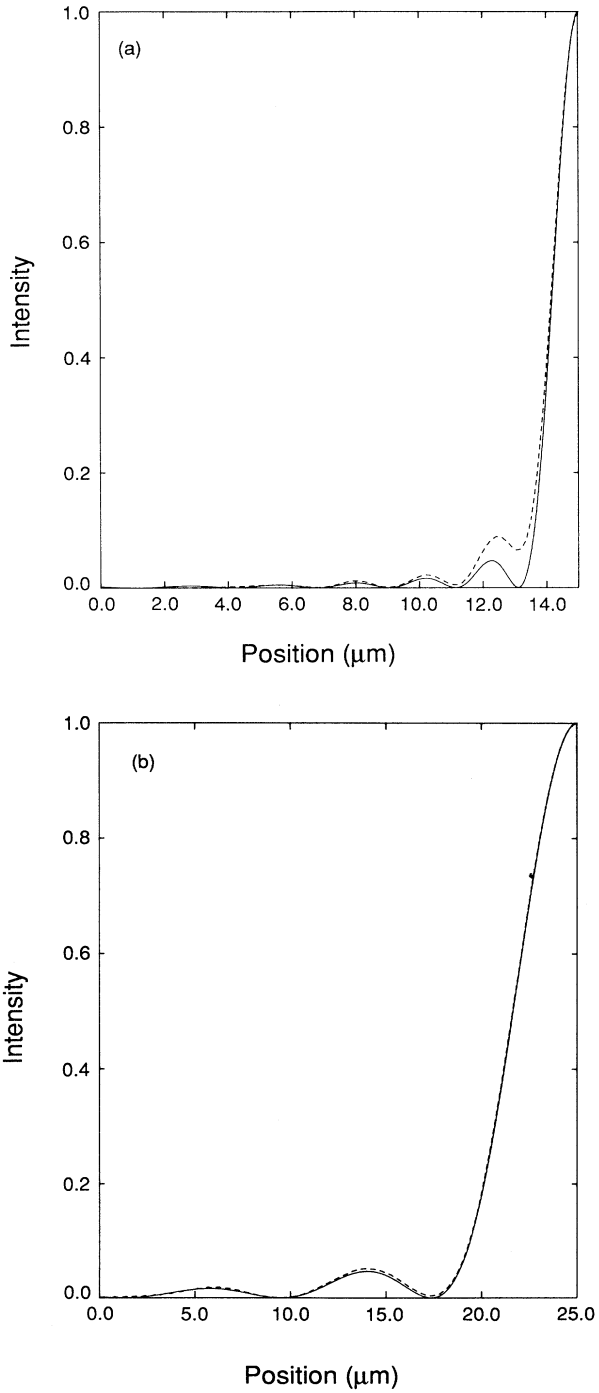

FIG. 5. Normalized intensity as a function of position (the device is symmetric about $L_y/2$) due to diffraction of 1-μm radiation by a 3-μm slit. The solid and dashed lines are the analytical Fraunhofer and Green's-function results, respectively. (a) Diffraction at a distance of 20 μm from the slit, and (b) diffraction at a distance of 80 μm from the slit.

determining the correct parameters for the absorbing boundary conditions is simplified. The volume grating is a 200 period first-order distributed-feedback reflector, where $n_g=3.6$, $n_{c1}=3.45$, and $n_{c2}=3.4$. The guiding region width of 0.1 μm was chosen to ensure single-mode operation in each of the waveguides. At a wavelength of 1.0 μm, the nominal effective index n_{eff} of the structure is 3.424 03; hence $\Lambda_1=\Lambda_2=\lambda/(4n_{\text{eff}})=0.073\,013$ μm. Figure 4 gives the reflectance of the grating as a function of wavelength, where the solid lines are the exact scattering matrix results [18] and the crosses are the recursive-Green's-function results. For the calculations, the input wave was taken to be the guided wave formed in the waveguide of thickness Λ_1. W_a and n_i were chosen such that the integrated input intensity equaled the total integrated output intensity, where the majority of results were generated with $W_a=2.9$ and $n_i=0.04$. Since the structure is symmetric about $L_y/2$, only half of the device was simulated; the transverse mesh employed 81 basis functions, while ΔL_z was 7.3013 nm (0.730 13 nm was also tried, yielding analogous results). For each wavelength, the calculation required $\sim$56 s on an IBM RS6000 workstation (the code has not been optimized). As can be seen from Fig. 4, the two results are nearly in perfect agreement. Since some recent BPM techniques [4,5] have difficulties modeling strongly guiding structures, a 50 period grating with n_{c1} and n_{c2} equal to 2.45 and 2.4, respectively, was simulated, yielding also nearly perfect agreement with the scattering matrix results.

In order to show that modeling of very large domains is possible, wave propagation through a single slit was simulated. In the simulation, a plane wave ($\lambda=1$ μm) was incident from a media with an index of 1.0 on a 3-μm slit, beyond which lay a media having an index of 3.5. Again, as a result of symmetry about $L_y/2$, only half of the device was simulated. Two domains were modeled, one with L_y and L_z equal to 30 and 20 μm, respectively, and the other with L_y and L_z equal to 50 and 80 μm, respectively. The results are shown in Figs. 5(a) and 5(b), respectively, where the solid lines are the Fraunhofer diffraction results [18], while the dashed lines are the Green's-function results. For L_z equal to 20 and 80 μm, the number of transverse basis functions was 106 and 140, respectively, and ΔL_z was 100 nm for both. For the 80-μm simulation, the calculation required $\sim$180 s on the IBM RS6000 workstation. Figure 5 shows that our results accurately reproduce the positions of the maxima and minima, and for the 80-μm simulation, the two curves are nearly coincident. Thus the far-field regime does not actually begin until $\sim$100 μm beyond the slit. For the 20-μm simulation, the final maxima around 3 μm is not present in the Green's-function results due to numerical noise.

IV. CONCLUSIONS

We have introduced an alternative technique for calculating wave propagation through nonhomogenous two-dimensional media. It is based on a recursive-Green's-function technique, which yields the exact Green's function for the problem domain. As a result, comparisons made with known analytical solutions yield effectively exact agreement. Besides its accuracy, the other major virtue of the approach is its reduction of a large two-dimensional problem into a series of one-dimensional ones. Consequently, the computational times are significantly faster than analogous calculations using the finite-difference time-domain method, enabling the simulation of larger and more complex structures.

ACKNOWLEDGMENT

We would like to thank J. P. Spence for helpful discussions.

[1] M. D. Feit and J. A. Fleck, Jr., Appl. Opt. **17**, 3990 (1978).
[2] Y. Chung and N. Dagli, IEEE J. Quantum Electron. **QE - 26**, 1335 (1990).
[3] M. Glasner, D. Yevick, and B. Hermansson, J. Opt. Soc. Am. B **8**, 413 (1991).
[4] D. Yevick, W. Bardyszewski, B. Hermansson, and M. Glasner, IEEE Photon. Technol. Lett. **3**, 527 (1991).
[5] R. P. Ratowsky and J. A. Fleck, Opt. Lett. **16**, 787 (1991).
[6] K. Hirayama and M. Koshiba, IEEE Trans. Microwave Theory Tech. **MTT - 37**, 761 (1989).
[7] B. M. Dillon, R. L. Ferrari, and T. P. Young, Electron. Lett. **26**, 47 (1990).
[8] K. S. Yee, IEEE Trans. Antennas Propag. **AP-14**, 302 (1966).
[9] G. Mur, IEEE Trans. Electromagn. Compat. **EMC-23**, 377 (1981).
[10] W. P. Huang, S. T. Chu, A. Goss, and S. K. Chaudhuri, IEEE Photon. Technol. Lett. **3**, 524 (1991).
[11] D. J. Thouless and S. Kirkpatrick, J. Phys. C **14**, 235 (1981).
[12] K. B. Kahen, IEEE J. Quantum Electron. (to be published).
[13] K. B. Kahen, J. Appl. Phys. **71**, 4577 (1992).
[14] E. N. Economou, *Green's Functions in Quantum Physics,* Springer Series in Solid State Sciences, Vol. 7 (Springer, New York, 1983), Chap. 4.
[15] H. Wyld, *Mathematical Methods for Physics* (Benjamin-Cummings, Reading, MA, 1976), Chap. 8.
[16] E. Butkov, Mathematical Physics (Addison-Wesley, Reading, 1968), Chap. 12.
[17] L. Lapidus and G. F. Pinder, *Numerical Solution of Partial Differential Equations in Science and Engineering* (Wiley, New York, 1982), Chap. 2.
[18] M. Born and E. Wolf, *Principles of Optics* (Pergamon, Oxford, 1980).